Elemental Analysis of Nanomaterial Using Photon-Atom Interaction Based EDXRF Technique

Sanjeev Kumar[1], Arun Kumar[2], Mansi Chitkara[3], I.S. Snadhu[3] and Devinder Mehta[2]

[1]G.G.D.S.D. College Sector-32, Chandigarh

[2]Department of Physics, Panjab University, Chandigarh

[3]Nanomaterials Research Laboratory, Chitkara University, Rajpura 140401, Punjab, India

Abstract   Presence of trace amount of foreign impurities (both metallic and non-metallic) in standard salts used for sample preparation and during the synthesis process can alter the physical and chemical behavior of the pure and doped nano-materials. Therefore, it becomes important to determine concentration of various elements present in synthesized nano-material sample. In present work, the elemental and compositional analysis of nano-materials synthesized using various methods has been performed using photon-atom interaction based energy dispersive x-ray fluorescence (EDXRF) technique. This technique due to its multielement analytical capability, lower detection limit, capability to analyze metals and non-metals alike and almost no sample preparation requirements can be utilized for analysis of nano-materials. The EDXRF spectrometer involves a 2.4 kW Mo anode x-ray tube (Pananalytic, Netherland) equipped with selective absorbers as an excitation source and an LEGe detector (FWHM = 150 eV at 5.895 keV, Canberra, US) coupled with PC based multichannel analyzer used to collect the fluorescent x-ray spectra. The analytical results showed good agreements with the expected values calculated on the basis of the precursor used in preparation of nano-materials.

1. INTRODUCTION

The improved understanding of nano-scale phenomena is critical for the advancement for the various applications in material science. Artificially created nano-structures, including metal and semiconductor nano-wires and nano-tubes have unique mechanical, magnetic, optical and thermoelectric properties. Since their discovery in 1991 [1], carbon nano-tubes (CNTs) have been the basis for various nanoscale devices such as field effect transistors [2–5], heterojunctions [6,7] and nanocomputing applications [8,9]. Nano-tubes can efficiently transport electrons with optical excitation via their interesting one-dimensional structures. Current fabrication methods yield nano-tubes with a range of diameters (~20-300 nm) and different rolling orientations, resulting in the unpredictability of producing metallic or semiconducting nano-tubes [10]. Controlling the diameter and chirality in the nanotubes is difficult. As the electric properties of one-dimensional semiconducting structure are controlled by their diameter [11], therefore these techniques are not suitable for nanotubes. Also, the controlled and long-term stable doping of nano-tube is very challenging. Nano-wires have been gaining a lot of attention as alternatives to CNTs because their growth is easier to control and have been relatively easier to dope with suitable impurities. Nano-tubes

Kumar, S.
Kumar, A.
Chitkara, M.
Snadhu, I.S.
Mehta, D.

and nano-wires of various materials can be synthesized using template-based approach and chemical methods. Different nano-structures are extensively characterized using techniques such as high-resolution Transmission Electron Microscopy (HR-TEM) and Field Emission scanning electron Microscopy (FE-SEM). The particle size and shape of the nano-structure material will be determined using x-ray diffraction (XRD) analysis. In addition, the elemental analysis and composition of the nano-structure material is further verified using x-ray emission techniques.

62

One of the important classes of techniques in elemental analysis is based on photon-atom interaction apart from nuclear reaction activation analysis and electron/ion-induced x-ray emission. Following photoionization of inner-shells, the emitted characteristic x rays or Auger electrons are measured, and used for identification and quantification of the elements. The energy dispersive x-ray fluorescence (EDXRF) technique [12–18], involving measurement of characteristic x rays from the sample using semiconductor detectors has been well established to determine the elemental concentrations of various elements simultaneously. In case of all the elements present in the sample emit fluorescent x rays detectable by semiconductor detectors, one can make use of the x rays to determine concentration of these elements in the sample and hence, thickness of the sample using EDXRF technique. The energy dispersive x-ray fluorescence (EDXRF) is a rapid, sensitive and non-destructive technique for providing semi-quantitative and qualitative information of the trace elements present in the sample. EDXRF technique cannot be used for elements whose low-energy characteristic x rays are not detectable by the generally available detectors. The elastic and inelastic scattering are other important modes of photon interaction with matter and also have applications in material characterization [12, 19, 20]. The elastic-scattering measurements in the x-ray energy region, i.e., below 100 keV can be used for Z-dependent characterization of materials, while the inelastic-scattered x rays can be used for measurements of several physical quantities such as electron density, target mass, and mass density. The RRS is still being explored for applications in chemical speciation of samples [21,22]. The other important point is that the attenuation cross-section (cm^2/g) in H is higher by a factor of ~2 as compared to that for other elements at photon energy above 20 keV. This is because mass of the atom is mainly contributed by the nucleons and scattering is mainly due to the electrons. For H, the ratio of number of electrons to number of nucleons is very different from the other elements. Hence, the information regarding attenuation of photons can be exploited to estimate abundance of H in hydrogen-rich samples [20]. This property can be used to measure H in hydrogen-rich compounds like paraffin wax target. The x-ray and γ-ray transmission methods are suitable for bulk thickness [12]. These can be used in conjunction with the EDXRF and supplement it for limited number of low-Z elements. At the low photon energies, photoionization is the major contributor to their attenuation in matter. Attenuation measurements have the advantage of being independent of enhancement type matrix effects observed in EDXRF analysis. The attenuation measurements require relatively less measurement time and weaker photon source. Furthermore, the energy resolution of the detector is not a limitation

Elemental Analysis
of Nanomaterial
Using Photon-
Atom Interaction
Based EDXRF
Technique

63

in such measurements. However, for measuring thickness of the low-Z sample or a sample with low-Z material used as coating and/or backing on a high-Z substrate, one can preferably make use of the attenuation of low energy photons. One should be careful regarding the RRS contribution to attenuation measurements at incident photon energies in the lower vicinity of the electron threshold of the element.

In the present work, the EDXRF technique and attenuation method have been used for analysis of nano-structures. The following measurements have been done (i) Measurements of Ag in thin PVA (polyvinyl alcohol) Ag nano-composite films and (ii) Elemental analysis of some template synthesized nano-wires and nano-tubes using EDXRF technique. These analyses are required to check the possibility of some contamination intruded left-over during synthesis of nano-materials.

2. MEASUREMENTS OF THIN AG NANO-PARTICLE FILMS

The PVA (Polyvinyl alcohol)-Ag nano-composite samples were prepared by the nanoscience group of the Physics Department, Kurukshetra University to study their optical and electrical properties. Ag nano-particles were prepared in water by chemical reduction of silver nitrate (0.01 M solution) with sodium borohydride (NaBH4, 0.001M solution). The 0.3% solution of PVP (Polyvinyl Pyrodine) solution is added as a stablising agent. Further, PVA-Ag nanocomposites were prepared by dissolving 2 gm of PVA in different volume of Ag colloidal. PVA-Ag films were prepared using sol-gel method and spin coating. TEM measurements were done for the size measurement of the Ag nano-particles prepared in water. Nano-particles were found relatively monodisperse and relatively spherical. The average size of the particles was found to be 20 nm ± 5 nm. To study the optical properties of the films, the concentration of Ag nano-particles in the prepared films is required.

3. GEOMETRICAL SET-UP AND MEASUREMENTS

The elemental and compositional analysis of the synthesized nano-material samples were carried out using the EDXRF spectrometer involving a 2.4 kW Mo anode x-ray tube (60 kV, water cooled, PW 2274/22, Pananalytic, The Netherlands) as a source of excitation. The background due to scattered photons was minimized by placing the x-ray tube, target sample and the detector in 90° reflection mode geometrical arrangement as shown in the Fig. 1. An LEGe detector in horizontal configuration (100 mm^2 × 10 mm, 8-µm Be window and FWHM = 150 eV at 5.895 keV, Canberra, US) coupled with PC based multichannel analyzer (Multiport II) was used to collect the fluorescent x-ray spectra from the samples. The target was mounted at 45° with the detector and x-ray tube axis. The x-ray tube and detector were kept outside the chamber. The alignment of the x ray tube collimator and chamber collimator was done using laser beam. The x-ray tube is generally operated at 29 kV to avoid excitation of the Sn-collimator with K-Shell binding energy, $B_K = 29.20$ keV and 10 mA. The take off angle of the tube window with respect to the horizontal direction is 6°. The spectra

Kumar, S.
Kumar, A.
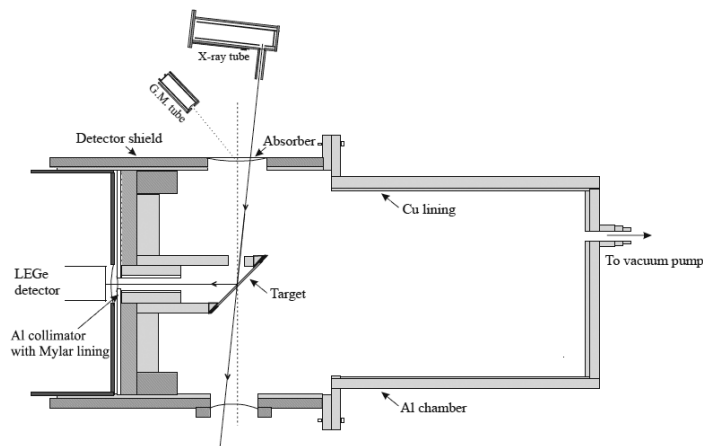Chitkara, M.
Snadhu, I.S.
Mehta, D.

64

Figure 1: Geometrical arrangement used for the Ag nano-composite thin film measurements.

for each sample were collected for the time periods of 2000 sec. The bremsstrahlung and Mo-Kβ (19.65 keV) x rays emitted from the x-ray tube was reduced by using Zr (70 mg/cm^2, B$_K$ = 18.986 keV) absorber. The Mo Kα (17.44 keV) x rays along with reduced bremsstrahlung were in turn used to excite the characteristic x-ray of elements present in the samples. A G.M. counter facing the incident beam absorber mounted on the chamber was used to monitor the incident beam flux from the x-ray tube. The thickness of the Ag-nano particle film was expected to be in the range 0.5-2.5 μg/cm^2. As the Mo x-ray tube has the intense Mo K x-rays and bremsstrahlung in the Ag K x-ray region, and Ag excitation is only by the bremsstrahlung, i.e., the detection limit was poor to detect 0.5 mg/cm^2 thick Ag target. To handle this problem, an absorber of $_{39}$Y (60 mg/cm^2) with B$_K$ = 17.038 keV was used to suppress the Mo Kα x rays and bremsstrahlung in the region of Ag K x rays. This has also significantly reduced the excitation bremsstrahlung. The tube voltage was increased so that the hump due to bremsstrahlung is moved to higher energy region, i.e., away from the region of interest. The x-ray tube was finally operated at 45 kV for the present measurements. This exercise resulted in improved peak-to-background ratio and observation of Ag Kα x-ray peak to become visible well above the background even for the thinnest available target ~0.5 g/cm^2 as shown in Figs. 2(a) and (b), respectively.

The Ag Kα x-ray spectra normalized for same time are shown in Fig. 3. The self absorption correction factors for the thickness of the targets are negligible for the incident photons and emitted Ag K x rays. Spectra for the standard Ag targets (thickness = 99 and 263 μg/cm^2; Micromatter, US) were also taken and used for deducing thickness of the Ag nano-particle films by unitary method.

Elemental Analysis
of Nanomaterial
Using Photon-
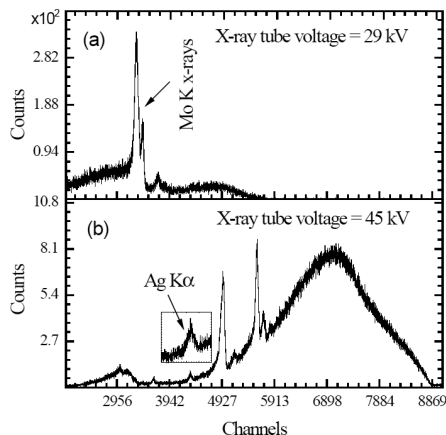Atom Interaction
Based EDXRF
Technique

65

Figure 2: Typical spectra for Ag nano-sample (a) using Mo anode x-ray tube at 29 KV (b) using Mo anode x-ray tube with 39Y absober at 45 KV.

4. EVALUATION PROCEDURE

The measured differential cross sections for the Ag Kα X-ray photons were evaluated using the relation

$$\left(\frac{d\sigma}{d\Omega}\right) = \frac{N}{4\pi I_o G \varepsilon m \beta} \tag{1}$$

where N is the number of counts/s under the Kα X-ray peak, $I_o G$ is the intensity of photons falling on the portion of target visible to the detector, ε is the detector efficiency keV, m is thickness of the target foil in g/cm², and β is the absorption correction factor which accounts for absorption of the incident and the elastic scattered photons in target. The values of absorption correction factors is given by expression

$$\beta_M^R = \frac{1 - \exp\left[-\left\{(\mu_{in}/\rho)_1 / \cos\theta_i + (\mu_{em}/\rho)_2 / \cos\theta_e\right\}m\right]}{\left\{(\mu_{in}/\rho)_1 / \cos\theta_i + (\mu_{em}/\rho)_2 / \cos\theta_e\right\}m} \tag{2}$$

where μ_{in} and μ_{em} are the attenuation coefficients (cm²/g) for the incident photons and emitted characteristic x-rays, respectively. θ_i and θ_e are the angles made by the incident and the scattered photons with the normal to the target surface. As all the spectra were taken under similar conditions, all the terms occurring in Eqn.1 except the count rate for the standard target and the nano-particle sample will cancel. The number of counts under the scattered part of the bremsstrahlung in the spectrum and x-ray counts from the G.M. tube was used to check the stability of the excitation spectrum. After analyzing the spectra for various nano-films, the concentration of Ag nano-particles were found to be 0.97%, 0.87%, 0.81% and 0.53% when 2 gm of PVA dissolved in 18 ml, 16 ml, 12 ml and 8 ml Ag colloidal solution respectively. The Amount of Ag present in
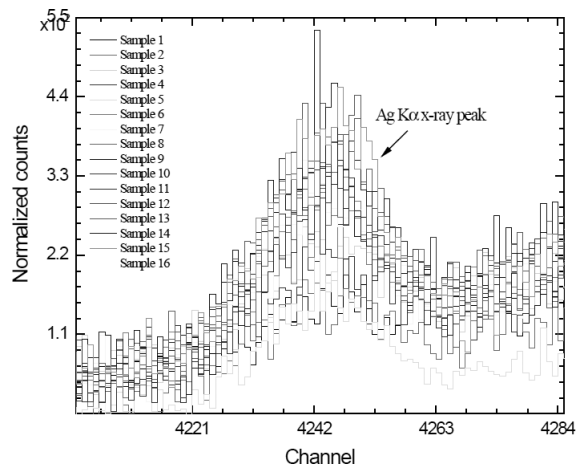
Kumar, S.
Kumar, A.
Chitkara, M.
Snadhu, I.S.
Mehta, D.

66

Figure 3: Normalized Spectra of Ag-composite nano-films taken with Mo anode x-ray tube.
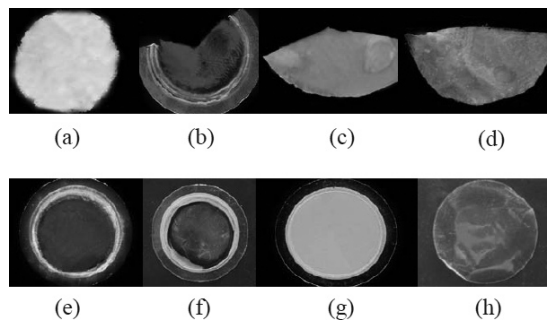

Figure 4: Photos of template synthesized (a) AgI, (b) Ag2S, (c) Ni, (d) Cu, (e) Se, (f) Cu2S nano-wires, (g) Al2O3 filter and (h) ion irradiated poly carbonate template.

various Ag nano-particle films are also summarized in Table 1. It is concluded that for the composite sample with lower Ag concentration one should use same portion of the sample for other kind of measurements like UV visible study, TEM measurements etc. to avoid the non-uniformity effects.

5. ELEMENTAL ANALYSIS OF SOME TEMPLATE SYNTHESIZED NANO-MATERIALS

The basic principle involved in template synthesized nano-materials is similar to that of producing components through the use of replication. In this technique; desired materials can be synthesized within the pores of the template membranes. If the
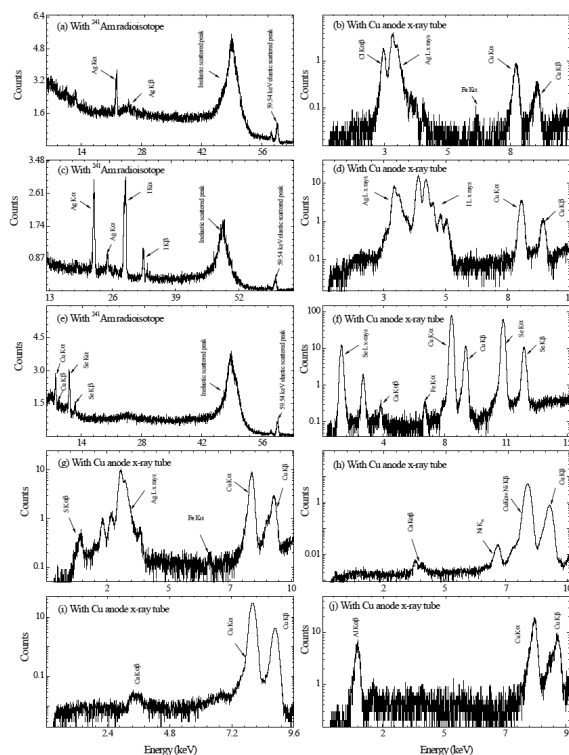
Elemental Analysis
of Nanomaterial
Using Photon-
Atom Interaction
Based EDXRF
Technique

67

Figure 5: The spectra of AgCl (a and b), AgI (c and d), CuSe (e and f), Ag2S (g), Ni nano-wires (h), Cu nano-wire (i) and Al2O3 j filter excited with 241Am and Cu anode x-ray tube.

templates that are used have cylindrical pores of uniform diameter, monodisperse nano-cylinders of desired material are obtained within the void of template material. Depending upon the operating parameters, these nano-cylinders may be solid (nano-wires) or hollow (nano-tube). The two basic technique used for the template synthesis of nano-materials are electrochemical deposition and electroless deposition. In the first technique, electrodeposition of a material within the pores of template membrane is obtained by coating one face of the template with a metal film and using same film a cathode for electroplating. The volume of the templates pores are uniformly filled with material and the length of nano-structure can be controlled by varying the amount of deposited materials. The latter technique involvesdeposition of material from the surrounding phase along the cylindrical pores walls of the template surface. After a short deposition times, a hollow tubule (nano-tubes) is obtained within each pore, whereas long deposition times results in solid nano-wires. The inside diameter of the nano-tubes can be controlled by varying the deposition time. After the pores are filled with the desired material, the replica is separated from the membrane matrix either by

Kumar, S.
Kumar, A.
Chitkara, M.
Snadhu, I.S.
Mehta, D.

68

Table 1: Amount of Ag present in various Ag nano-particle films.

Ag nano-samples	Amount of solution taken (in ml)	Amount of Ag particles (in %)
Sample 1	2	0.24%
Sample 2	4	0.44%
Sample 3	6	0.52%
Sample 4	8	0.53%
Sample 5	10	0.79%
Sample 6	12	0.81%
Sample 7	14	0.87%
Sample 8	16	0.87%
Sample 9	18	0.97%
Sample 10	20	0.97%
Sample 11	22	0.21%
Sample 12	24	1.22%
Sample 13	26	1.27%
Sample 14	28	1.36%

Table 2: Characteristics of nano-wires used in the present measurements.

S.N.	Sample used (nano-wires)	Template used	Synthesized technique	Salt used in prepration	Solvant materials
1.	Cu	ITM	Electro-deposition	$CuSO_4.5H_2O$, H_2SO_4	H_2O
2.	Ni	ITM	Electro-deposition	$NiSO_4.5H_2O$, H_3BO_3	H_2O
3.	AgI	ITM	Electro-deposition	$AgNO_3$, KI	H_2O
4.	Ag	Al_2O_3 filters	Electroless	$AgNO_3$	H_2O
5.	Se	Al_2O_3 filters	Electro-deposition	SeO_2, H_3BO_3	H_2O
6.	Ag_2S	Al_2O_3 filters	Electroless	$AgNO_3$, Na_2S	H_2O

peeling it off mechanically or by dissolving the membrane itself in suitable solvent [23,24]. More details about template, salt and solvent used for nano-wire preparation is given in Table 2. Among the various host template membranes, ITMs (ion track membranes) act as very good templates for the fabrication of nano/microstructures having desired shape and size [25,26]. The synthetic template involves heavy ion irradiated polymeric foil followed by etching of induced latent tracks by suitable solvent leads to formation of nearly cylindrical pores. Some template synthesized nano-wires used in present measurements are shown in Fig. 4 and typical spectra of each nano-wires and template used as samples are shown in Figs. 5 (a)-(j).

6. EXPERIMENTAL SET-UPS AND MEASUREMENTS

The elemental and compositional analysis of template synthesized nano-material samples were carried out using two EDXRF spectrometers as shown in Fig. 1. The low-Z elemental

analysis was done using EDXRF set-up involved a 2.5 kW copper anode x-ray tube (Pananalytic made, PW 2274/22, 60 keV, water cooled) as a source of excitation. The x-ray tube was operated at 20 kV and 5 mA. The bremstrahlung emitted from the x-ray tube was reduced by using Ni (20 mg/cm2) absorber. The Cu Kα (8.041 keV) and Kβ (8.907 keV) x-ray along with reduced bremsstrahlung were in turn used to excite the characteristic x-ray of elements present in the samples. An LEGe detector in horizontal configuration (100 mm2 × 10 mm, 8-μm Be window and FWHM = 150 eV at 5.895 keV, Canberra, US) coupled with PC based multichannel analyzer (Multiport II) was used to collect the fluorescent x-ray spectra from the samples. The background due to scattered photons was further minimized by placing the x-ray tube, target sample and the detector in 90° reflection mode geometrical arrangement as shown in the Fig. 1. The spectra for each sample were collected for the time periods of 5000 sec. The high Z nano-material samples were also analyzed using the reflection mode geometrical arrangement involving the [241]Am annular-source and Al-lined Pb collimator. The LEGe detectors were used to detect the characteristic x rays emitted from the sample.

7. CONCLUSION

Different aspects of photon-atom based techniques to analyze samples related to nanomaterials are discussed. The EDXRF technique can be used to measure thickness of the PVA-nano-particle composite films required by the Nano-Scientists of the region. The detection limit in the x-ray tube set-up can be improved considerably by using (i) absorbers in front of the x-ray tube to selectively absorb the incident photon flux of in the energy range of interest, and (ii) by selecting the x-ray tube voltage so that hump due to Bremsstrahlung in the spectrum as well as its Ge K x-ray escape is moved away from the region of interest. The composition and purity of the nano-particles prepared using template-based methods was also checked using EDXRF technique.

REFERENCES

[1]   C.S. Iijima, Nature **354,** 56 (1991). http://dx.doi.org/10.1038/354056a0

[2]   S.J. Tans, A.R.M. Verschueren and C. Dekker, Nature **393,** 49 (1998).
        http://dx.doi.org/10.1038/29954

[3]   J.A. Misewich, R. Martel, P. Avouris, J.C. Tsang, S. Heinze and J. Tersoff, Science **300,** 783 (2003). http://dx.doi.org/10.1126/science.1081294

[4]   K. Liu, M. Burghard, S. Roth and P. Bernier, Appl. Phys. Lett. **75,** 2494 (1999).
        http://dx.doi.org/10.1063/1.125059

[5]   Y. Huang, X.F. Duan, Y. Cui and C.M. Lieber, Nano Lett. **21,** 01 (2002).

[6]   M.S. Fuhrer, J. Nygard, L. Shih, M. Forero, Y.G. Yoon, M.S.C. Mazzoni, H.J. Choi, J. Ihm, S.G. Louie, A. Zettl and P. L. McEuen, Science **288,** 494 (2000).
        http://dx.doi.org/10.1126/science.288.5465.494

[7]   Z. Yao, H.W.C. Postma, L. Balents and C. Dekker, Nature **402,** 273 (1999).
        http://dx.doi.org/10.1038/46241

[8]   Y. Huang, X.F. Duan, Y. Cui, L.J. Lauhon, K.H. Kim and C. M. Lieber, Science **294 ,** 1313 (2001). http://dx.doi.org/10.1126/science.1066192

[9]   M.R. Diehl, S.N. Yaliraki, R.A. Beckman, M. Barahona and J.R. Heath, Angew. Chem. Int. Ed. **41,** 353 (2002). http://dx.doi.org/10.1002/1521-3773(20020118)41:2<353::AID-ANIE353>3.0.CO;2-Y

[10]   P.C. Collins, M.S. Arnold and P. Avouris, Science **292,** 706, (2001). http://dx.doi.org/10.1126/science.1058782

[11]   J.T. Hu, L.S. Li, W.D. Yang, L. Manna, L.W. Wang and A.P. Alivisatos, Science **292,** 2060 (2001). http://dx.doi.org/10.1126/science.1060810

[12]   R. Cesareo, Nucl. Instrum. and Meth. B **150,** 571 (1999). http://dx.doi.org/10.1016/S0168-583X(98)01062-3

[13]   S. Puri, J.S. Shahi, B. Chand, M.L.Garg, Nirmal Singh and P.N. Trehan, X-ray spectrometry **27,** 105 (1998). http://dx.doi.org/10.1002/(SICI)1097-4539(199803/04)27:2<105::AID-XRS258>3.0.CO;2-W

[14]   S. Kumar, S. Singh, D. Mehta, M.L. Garg, P.C. Mangal and P.N. Trehan, X-ray spectrometry **18,** 207 (1989). http://dx.doi.org/10.1002/xrs.1300180505

[15]   A.G. Karydas and T. Paradellis, X-ray spectrometry **22,** 208 (1993). http://dx.doi.org/10.1002/xrs.1300220408

[16]   F.J. Pantenburg, T. Beier, F. Hennrich and H. Mommsen, Nucl. Instrum. and Meth. **B 68,** 125 (1992). http://dx.doi.org/10.1016/0168-583X(92)96063-5

[17]   V.D. Martinez, C.M. Hidalgo and R.A. Barrea, X-ray spectrometry 29, 245 (2000). http://dx.doi.org/10.1002/(SICI)1097-4539(200005/06)29:3<245::AID-XRS429>3.0.CO;2-O

[18]   M. Manter and M. Schreiner, X-ray spectrometry **29,** 3 (2000). http://dx.doi.org/10.1002/(SICI)1097-4539(200001/02)29:1<3::AID-XRS398>3.0.CO;2-O

[19]   R. Speller, X-ray spectrometry **28,** 22 (1999). http://dx.doi.org/10.1002/(SICI)1097-4539(199907/08)28:4<224::AID-XRS343>3.0.CO;2-F

[20]   K. Molt and R. Schramm, X-ray spectrometry **28,** 22 (1999). http://dx.doi.org/10.1002/(SICI)1097-4539(199901/02)28:1<59::AID-XRS310>3.0.CO;2-N

[21]   K.E. Miyano, Y. Ma, S.W. Southworth, P.L. Cowan and B.A. Karlin, Phys. Rev. **B 54,** 12022 (1996). http://dx.doi.org/10.1103/PhysRevB.54.12022

[22]   Y. Udagawa and K. Tohji , Chem. Phys. Lett. **148,** 101 (1988). http://dx.doi.org/10.1016/0009-2614(88)80283-5

[23]   L.D. Pra, E. Ferain, R. Legras and S.D. Champagne, Nucl. Instr. and Meth. B 196, 81.

[24]   M. Sima, I. Enclescu, C. Trautmann and R. Neumann, J. Optoelec. & Adv. Mater. **6,** 121 (2004).

[25]   B.E. Fischer and R. Spohr, Rev. Mod. Phys. **55,** 907 (1983). http://dx.doi.org/10.1103/RevModPhys.55.907

[26]   M.E.T. Molares, E.M. Hohberger, C. Schaeflein, R.H. Blick, R. Neumann and C. Trautmann, Appl. Phys. Lett. **82,** 2139 (2003). http://dx.doi.org/10.1063/1.1563741